Analysis of the thermal field of electric power equipment

Dušan Medveď, Zsolt Čonka, Michal Kolcun
Department of Electric Power Engineering
Technical University in Košice
Košice, Slovakia
Dusan.Medved@tuke.sk , Zsolt.Conka@tuke.sk , Michal.Kolcun@tuke.sk

***Abstract*—The submitted paper deals with the analysis of the temperature field of selected electric power equipment. In the introduction there are described theoretical knowledge of thermodynamics, such as heat generation, influence of temperature increasing and heat transfer mechanisms. In the next sections, there are presented the results of simulations of temperature field distribution of selected electric power equipment using the ANSYS tool.**

Keywords—transformer, asynchronous motor, allowed warming, allowed temperature, heat, bended transformer station

I. INTRODUCTION

By passing the electric current through the conductor, the temperature of conductor increases and simultaneously hot conductor heats its nearest surroundings. Every temperature that exceeds the operational temperature, whether we talk about wires or electric machines, degrades the insulation, the wires and the device itself. In this paper we are addressing the solution of the temperature field distribution in the vicinity of three selected equipment: asynchronous motor, transformer and the bended octagonal transformer station.

The alternating electric current generates losses in electrical devices in its electric and magnetic circuit. Due these electric losses there is generated heat that increases the temperature of the device itself. If sufficient residual heat removal is not ensured, this can lead to subsequent damage, destruction of such devices. Therefore, for electrical devices, the maximum warming limits are set, which cannot be exceeded.

II. MECHANISMS OF HEAT TRANSFER

Assume that in specific space is inhomogeneously distributed temperature, then a heat transfer process takes place in this space. According to the second thermodynamic law, this process is carried out in the direction of the temperature drop, i.e. from the warmer to the colder area. This heat exchange process is characterized by a vector variable – the heat flux density vector q, which represents the amount of heat in joules passing through the surface unit [2].

For simplicity, it is possible to say that heat transfer is accomplished by three mechanisms: conduction; convection; radiation [2].

A. Conduction heat transfer

With heat transfer by conduction, we can meet when one would heat a rigid body (for example a metal rod). The molecules of the heated one end of the rod are wobbled around their equilibrium positions by the action of a heat source and gradually transfer energy to the neighboring molecules until the average kinetic energy of the molecules throughout the whole body is the uniform. Since the temperature is defined as the mean kinetic energy of the molecules, the rod is gradually heated from one end to the other. Heat transfer is considered to be a transfer in which the body molecules do not change their positions, the body does not move as such, there is no macroscopic movement [3].

B. Convection heat transfer

When heating the liquid in a glass container, one may notice moving the hot liquid up and dropping the cool liquid down. By stirring as a result of these movements, the temperature in the glass vessel is balanced and even when the heat is brought from the bottom, the fluid at the top surface is heated. Such heat transfer, which involves the macroscopic movement of the substance, i.e. mass convection, we say convection [3].

C. Radiation heat transfer

The sun is millions of kilometers away from us, but we can still feel its glow on us. Thermal energy comes to us from the sun through a thin environment, that is, essentially without a matter carrier. Solar energy is the energy of an electromagnetic field that we can see as waves or photons flow. Radiation can be observed almost on every subject that radiates heat whether it is a filament lamp or a burning coal. The heat radiates from each body having a temperature greater than 0 K [3].

III. MODELING OF TEMPERATURE FIELD AROUND THE ELECTRIC POWER DEVICE DURING THE OPERATION

The ANSYS software tool was used to model the temperature field distribution. ANSYS is a simulation software package that uses finite element method (FEM) for the calculations. The method provides a fairly solution accurate results. The method FEM commonly divides task/problem into a number of small parts with the finite number, which then comprise the set of algebraic equations.

A. Temperature field distribution modeling and analysis of a 3-phase asynchronous motor

The dimensions of the motor were measured by measuring of the individual parts of the real asynchronous electric motor with the designation Sg90L-4, which was disassembled for this purpose. The modeling began from the rotor shaft on which the rotor blades are rotor cage winding grooves. Next, there was proceeded by modeling the stator with the number of grooves $Q_{m2} = 36$. The stator yoke is made of stator sheets in which the winding is stored. Winding from stator sheets is separated by insulation. The stator winding is, unlike the rotor winding where the rods are used, made of wires. In the simulation, the stator winding

978-1-7281-1154-4/18/$31.00 ©2018 IEEE

was made as a pole for simplicity, and in order to reduce the computational difficulty, the individual phase poles were not interconnected (Fig. 1).

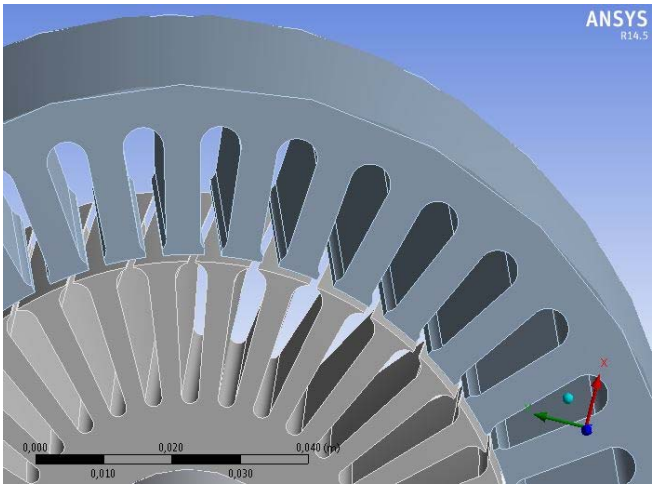

a)

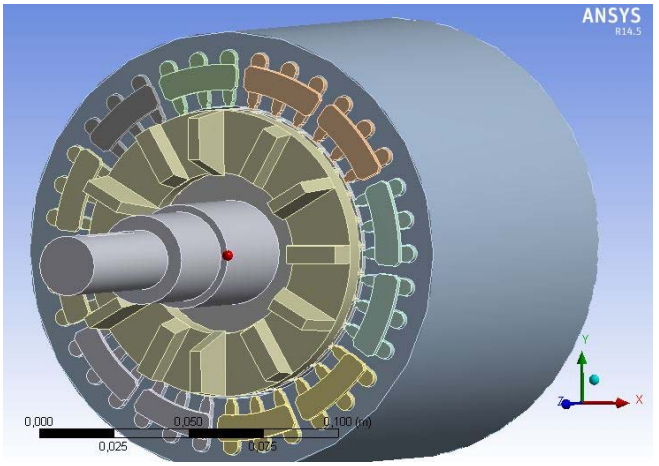

b)

Fig. 1. The rotor and stator body a) without winding, b) with windings

After modeling of all parts of the engine, including the shell, there was simulated asynchronous motor with the "enclosure" function that was placed in an air case of cuboid shape. Simulation took place in this space (Fig. 2).

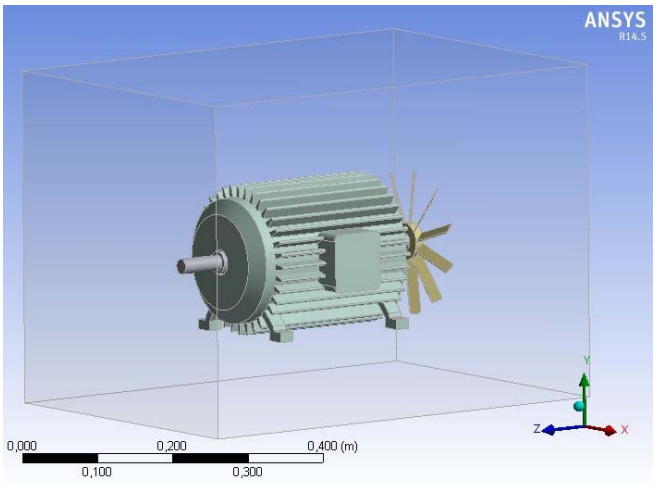

Fig. 2. Motor placed in an air enclosure

Once the geometry has been finished, the ANSYS has created a network (mesh) from the elements that serve to assemble the equations. Throughout the enclosure, the convection value was set to 2 $W \cdot m^{-2}$ °C. This condition ensures that the surface of each body radiates the energy of 2 W from the surface unit at a temperature difference of 1 °C. This has ensured a more even distribution of the temperature field and the interaction between gas and solid.

Total losses are the sum of losses: losses in iron, losses in the stator winding and in the rotor cage, and mechanical losses.

$$\Delta P = \Delta P_{\mathrm{Fe}} + \Delta P_{\mathrm{j1}} + \Delta P_{\mathrm{j2}} + \Delta P_{\mathrm{mech}} + \Delta P_{\mathrm{d}} = 63 + 92,473 + \\ +107,249 + 12,3 + 7,5 = 282,486 \text{ W} \quad (1)$$

In order to enter the given values of losses of stator windings, rotor windings, stator and rotor plates, it is necessary to convert them to volume quantities so that they can be input into simulation as the individual transformer elements by selecting "Internal Heat Generation".

Energy emitted from the stator iron:

$$q_{\mathrm{Fe,stat}} = \frac{\Delta P_{\mathrm{Feh}}}{V_{\mathrm{stat}}} = \frac{57,25}{8,6836 \cdot 10^{-4}} = 65928,877 \text{ W} \cdot \text{m}^{-3} \quad (2)$$

the calculated internal heat source (2) was applied on the stator plates.

Energy emitted from the stator windings:

$$q_{\mathrm{j1stat}} = \frac{\Delta P_{\mathrm{j1}}}{V_{\mathrm{stat}}} = \frac{92,437}{4,035 \cdot 10^{-4}} = 229087,980 \text{ W} \cdot \text{m}^{-3} \quad (3)$$

the calculated internal heat source (3) was assigned to the stator winding.

Energy radiated from the rotor sheets (iron):

$$q_{\mathrm{Fe,rot}} = \frac{\Delta P_{\mathrm{mech}} + \Delta P_{\mathrm{d}} + \Delta P_{\mathrm{v}}}{V_{\mathrm{rot}}} = \frac{12,3 + 7,5 + 5,725}{5,1993 \cdot 10^{-4}} = 49093,147 \text{ W} \cdot \text{m}^{-3} \quad (4)$$

the calculated internal heat source (4) was applied on the rotor plates.

Energy emitted from the cage of the rotor:

$$q_{\mathrm{j2rot}} = \frac{\Delta P_{\mathrm{j2}}}{V_{\mathrm{rot}}} = \frac{107,249}{3,5399 \cdot 10^{-4}} = 302971,835 \text{ W} \cdot \text{m}^{-3} \quad (5)$$

the calculated internal heat source (5) was assigned to the rotor winding.

The ambient temperature in this simulation was set to $\vartheta_0 = 22$ °C, which is the common temperature for the interior applications of the asynchronous motor.

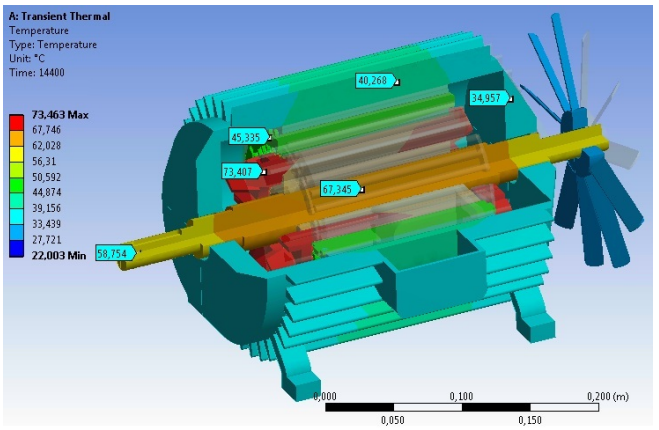

Fig. 3. Distribution of temperature field of the motor

The motor operator comes in contact mostly with the asynchronous motor cover, the surface of which during the operation at nominal load has temperature of 40.3 °C according to simulation, which is only slightly higher than the temperature of the human body. Such a touch does not present a risk of injury, does not cause the burn injuries. The maximum measured temperature was $\vartheta_{max1} = 73{,}463$ °C, in the rotor cage wires, maximum warming did not exceed the allowed warming $\Delta\vartheta_{dovF} = 105$ °C. The allowed warming condition was therefore respected. Cooling was sufficient, even if forced circulation was not ensured. However, regular maintenance of the actual cooling during the operation, i.e. fan control, cooling grid, and cleaning of sediments on cooling rigs are beneficial for extending the life of the electric machine.

B. Temperature field distribution modeling and analysis of dry distribution transformer 22/0.4 kV

In the transformer model, the iron core was first created. In order to optimize the calculation, the core was not made from individual sheets but from one solid piece of metal. Next, a secondary coil wound on the core, which is of the profile shape conductor of the rectangular cross section, was followed. Primary winding had a circular cross section, but it was not possible to produce an accurate primary winding model with actual winding thread design due to weak computer performance (PC workstation, 12-cores, 96 GB RAM).

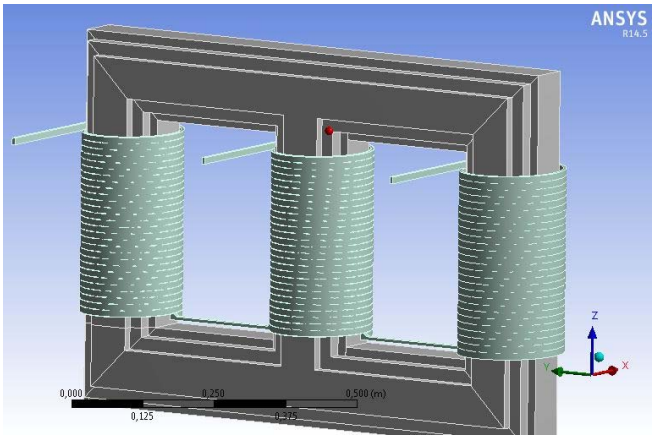

a)

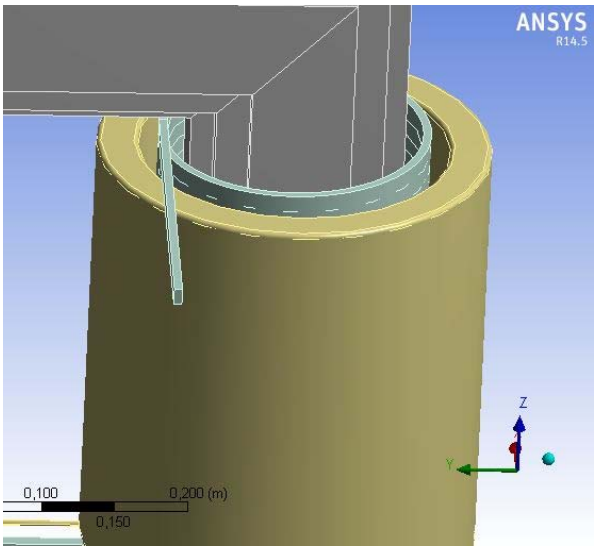

b)

Fig. 4. Transformer modeling a) secondary winding b) primary winding

In order to achieve the results as accurate as possible, the primary winding was simplified. The value of the volume that the wounded conductor occupied was only slightly different from the volume involved in the primary winding in the simulation.

Similarly, to the asynchronous motor, the transformer was modeled and was placed into air enclosure of cuboid shape. This enclosure represents the housing where the transformer was located. Its dimensions are 1130 × 1470 × 830 mm. In this space bordered by air enclosure there was realized simulation. Border and boundary conditions were set similarly to simulated asynchronous motors.

Total losses represent the sum of losses (3-ph) in the primary coil, secondary coil and losses in the iron core.

$$\Delta P_C = 3\cdot\Delta P_{11Al} + 3\cdot\Delta P_{21Al} + \Delta P_{Fe} = \\ = 4068{,}3 + 3628{,}8 + 1221{,}1 = 8918{,}2 \text{ W} \quad (6)$$

The calculated losses must be converted to volume to be entered for the individual elements of the transformer by selecting “Internal Heat Generation” (as in the previous case, for an asynchronous motor). The ambient temperature in this simulation was set to $\vartheta_0 = 22$ °C.

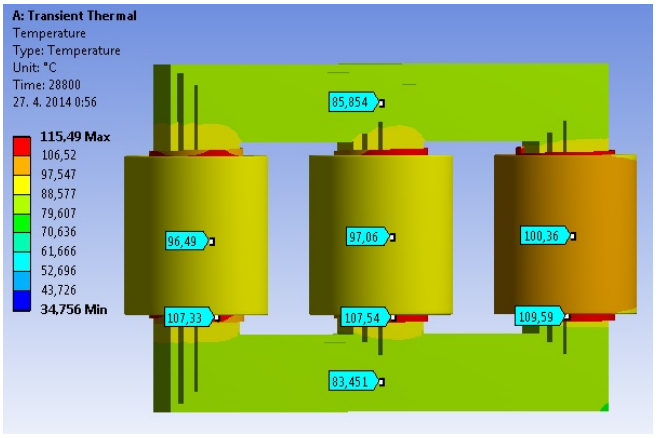

Fig. 5. Temperature field distribution in transformer 22/0,4 kV (8 hours)

The maximum measured temperature was ϑ_{max1} = 115.49 °C, on the secondary winding. This is due to the low flow of the flowing air and also to the large value of the drawn current. The compliance with the maximum warming limit has been met. Therefore, the cooling was sufficient, but if the ambient temperature rises above the set maximum ambient temperature ϑ_{40} = 40 °C, the transformer temperature will be ϑ_{max1} = 135,49 °C, which is close to the maximum allowable temperature for Class F insulation, i.e., ϑ_{dovF} = 155 °C. It is therefore recommended to apply active cooling of the transformer, which will extend the life of the transformer and reduce losses.

Design of additional active cooling

For this case, assume that during 1 hour of transformer operation, the heat of the transformer will be equal to Q_{loss}.

$$Q_{loss} = \Delta P_C \cdot t = 8918{,}2 \cdot 3600 = 321{,}055\,\text{MW}\cdot\text{s} = 321{,}055\,\text{MJ} \quad (7)$$

where t = 3600 s.

If we neglect the heat that is needed to heat the windings and the iron core, and we assume that all the heat that is generated by the passage of the current will be the heat that heats the air, we can determine the volume of air that will be heated by this warming with the desired warming of $\Delta\vartheta_{des}$. Consider warming from 22 °C to 85 °C, which means warming $\Delta\vartheta$ = 63 °C.

Then from the heat calculation formula Q we can obtain:

$$Q = c_{air} \cdot m_{air} \cdot \Delta\vartheta \quad (8)$$

where c_{air} = 1003 J·kg^{-1}·K^{-1} is the specific heat capacity of the air, m_{air} is the mass of air.

Then, the volume of air V_{air} is expressed from the air mass relation $m_{air} = \rho_{air} \cdot V_{air}$, and air volume that is heated in an hour:

$$V_{air} = \frac{Q}{c \cdot \Delta\vartheta \cdot \rho_{air}} = \frac{8918{,}2 \cdot 3600}{1{,}003 \cdot 10^3 \cdot 63 \cdot 1{,}2047} = 421{,}754\,\text{m}^3 \quad (9)$$

where ρ_{air} = 1,2047 kg·m^{-3} is the mass density of air at 20 °C.

Heat Q_{loss} heats air with volume V_{air} = 421,754 m^3 from temperature ϑ_1 = 22 °C to ϑ_2 = 85 °C. Since we assumed that the loss of ΔP_c is spent as heat in one hour, we can say that in order to maintain a constant value of warming during normal operation, we need to ensure that the air around the transformer is heated at a volume of at least 422 m^3 per hour. Thus, we get an air flow value of 422 m^3·h^{-1}, resp. 0,117 m^3·s^{-1} flowed through a ventilation device that drains the heated air out of the transformer case and provides the required supply of cool ambient air for cooling.

C. Temperature field distribution modeling and analysis of the bended octagonal transformer station 22/0,4 kV, 400 kW

The base of the transformer station model is an 8-angle (octagonal). As the height increases, the cross-section decreases. The mast is made of structural steel.

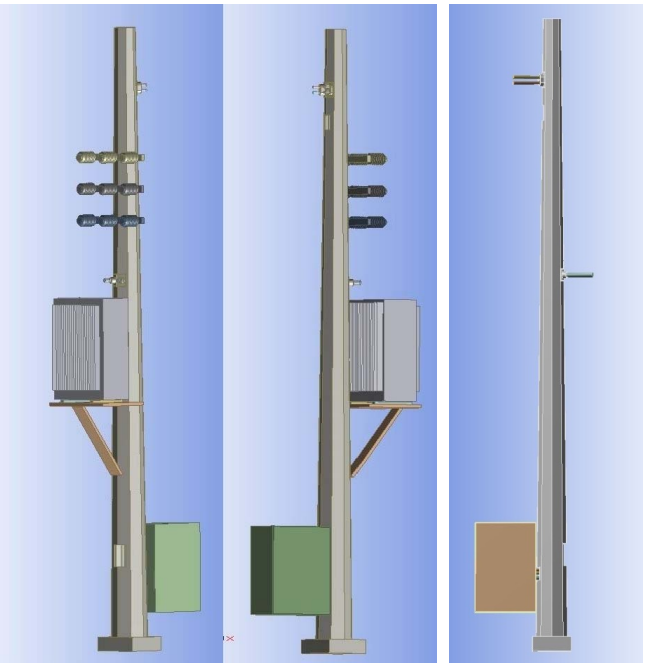

a)

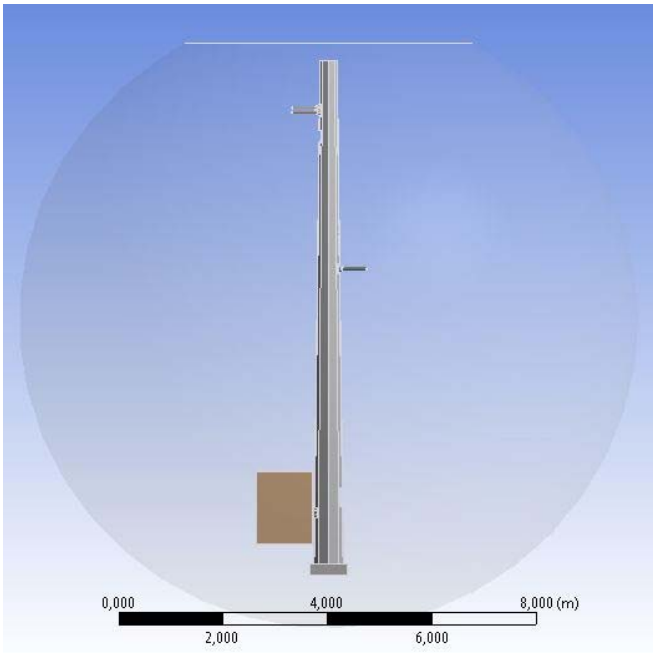

b)

Fig. 6. The rotor and stator body a) without winding, b) with windings

Due to the complexity of the calculation, the elements of the pole substation that did not affect the temperature field inside the pole were removed to simplify the geometry. The protective leakage pipes, which were located in the shaft of the pole, have also been removed. The transformation station was placed in an air enclosure of the sphere shape which was cut off at the top.

Total losses of the transformer station consisted of losses in leakage and terminal conductors for overhead power line:

$$\Delta P_C = 2 \cdot \Delta P_{CYKY} + 4 \cdot \Delta P_{NAYY} = 668{,}122\,\mathrm{W} \quad (10)$$

Calculated losses had been converted to volume quantities so that they can be entered for individual transformer elements by selecting option "Internal Heat Generation".

Energy emitted from the conductor 1-CYKY-J 4×120:

$$q_{CYKY} = \frac{\Delta P_{CYKY}}{V_{CYKY}} = \frac{109{,}991}{3 \cdot 240 \cdot 10^{-6} \cdot 5{,}946} = 25688{,}652\,\mathrm{W \cdot m^{-3}} \quad (11)$$

the calculated internal heat source (11) was applied for conductors $CYKY_1$ and $CYKY_2$.

The energy emitted from the conductor NAYY-J 4×120:

$$q_{NAYY} = \frac{\Delta P_{NAYY}}{V_{NAYY}} = \frac{112{,}035}{3 \cdot 120 \cdot 10^{-6} \cdot 8{,}785} = 35425{,}773\,\mathrm{W \cdot m^{-3}} \quad (12)$$

the calculated internal heat source (12) was entered for conductors $NAYY_1$, $NAYY_2$, $NAYY_3$ a $NAYY_4$.

The ambient temperature in this simulation was set to $\vartheta_0 = 30$ °C, which is the temperature during the summer days.

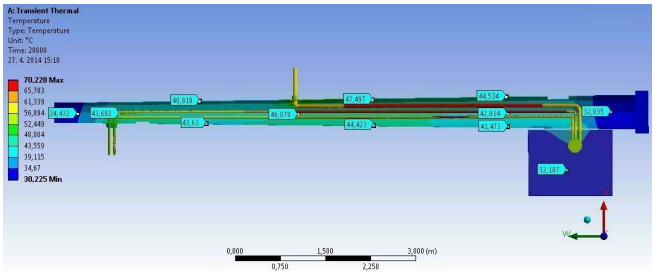

Fig. 7. Transformation station in cross section with temperatures of metal construction after 8 hours of operation (Note: figure of the pole was rotated in 90° due to minimalize place of this paper)

The conductor's temperature was assumed to be the highest in the lower third of the pole height. In the arrangement under consideration, there are six conductors which are directly heated by the transmitted current and heated indirectly from one another. The temperature of the conductor core NAYY-J was ϑ_{NAYY} = 70,2 °C. The conductor CYKY-J had a temperature of ϑ_{CYKY} = 67,8 °C. The operating temperature indicated by the manufacturer for these conductors was 70 °C. In the simulation, this temperature is somewhat higher (0,2 °C) so it is necessary to realize conditions for cooling or operate the bended transformer station bellow the nominal values of allowable current.

IV. Conclusion

This paper was devoted to the solution of the distribution of the temperature field around the selected electric power equipment (asynchronous motor, transformer and the bended octagonal transformer station). When analyzing the temperature field, it was taken into account that no overheating and degradation of the electrical as well as the thermal insulation properties of the individual parts of the equipment would occur. As a result of the increased temperature, destruction of the device may occur. Therefore, it is important to choose the right insulation with the appropriate temperature class, dimensioned for the intended warming. Of course, allowing the warming and the allowed temperature must not exceed the limit values. Any exceeding of this value reduces the life of the insulation and hence the device itself. Every 10 °C, above the allowed temperature, reduces the machine life by half. This means that lowering the temperature increases the life of the devices themselves. Therefore, it is necessary to continually sensing temperatures, warming and their subsequent reduction, for example by modifying the structure or by adding supplementary cooling.

Acknowledgment

This work was supported by the Ministry of Education, Science, Research and Sport of the Slovak Republic and the Slovak Academy of Sciences under the contract No. VEGA 1/0372/18.

References

[1] D. Medveď, O. Hirka, "*Investigation of Electromagnetic Fields in Residential Areas*", In: Acta Electrotechnica et Informatica. Vol. 17, No. 3 (2017), p. 48-52. ISSN 1335-8243.

[2] D. Medveď, M. Beluščák, J. Zbojovský, "*Solution of thermal field around transformer*". In: Elektroenergetika 2015. Košice: TU, 2015 p. 140-143. ISBN 978-80-553-2187-5.

[3] P. Liptai, et. al., "*Check measurements of magnetic flux density: Equipment design and the determination of the confidence interval for EFA 300 measuring devices*", In: Measurement. Vol. 111 (2017), p. 51-59. ISSN 0263-2241.

[4] L. Mišenčík, D. Medveď, "*Design of Dry Transformer Cooling*". In: Elektroenergetika. Vol. 6, No. 3 (2013), p. 28-31. ISSN 1337-6756.

[5] M. Pavlík, et. al., "*The impact of electromagnetic radiation on the degradation of magnetic ferrofluids*", In: Archives of Electrical Engineering. Vol. 66, no. 2 (2017), p. 361-369. ISSN 1427-4221.

[6] Forced Laminat Flow Over an Isothermal Plate. [online]. [cit. 2018-08-20]. Available at: <https://www.efunda.com/formulae/heat_transfer/convection_forced/calc_lamflow_isothermalplate.cfm>.

[7] J. Zbojovský, M. Pavlík, "*Calculating the shielding effectiveness of materials based on the simulation of electromagnetic field*", In: Elektroenergetika 2017. Košice: TU, 2017 p. 369-372. ISBN 978-80-553-3195-9.

[8] J. Kurimský, R. Cimbala, I. Kolcunová, "*Multi-scale decomposition for partial discharge analysis*", In: Przeglad Elektrotechniczny. Vol. 84, no. 9 (2008), p. 169-173. ISSN 0033-2097.

[9] R. Cimbala, J. Király, M. German-Sobek, S. Bucko, J. Kurimský, J. Džmura, "*Polarization Phenomena in Magnetic Liquids*", Chemicke listy 109, No. 2 (2015), 117–124. ISSN 2336-7202.

[10] J. Petráš, J. Kurimský, J. Balogh, R. Cimbala, J. Džmura, B. Dolník, I. Kolcunová, "*Thermally Stimulated Acoustic Energy Shift in Transformer Oil*", In: Acta Acoustica United with Acustica, Vol. 102 Issue: 1 Pages: 16-22, ISSN 1610-1928.

[11] M. Pavlík, et. al., "*Measuring of Dependence of Shielding Effectiveness of Wet Materials on The Frequency of Electromagnetic Field in the High Frequency Range*", In: Acta Electrotechnica et Informatica. Vol. 13, No. 3 (2013), p. 12-16. ISSN 1335-8243.

[12] M. Rajnak, B. Dolnik, J. Kurimsky R. Cimbala, P. Kopcansky, M. Timko, "*Electrode polarization and unusual magnetodielectric effect in a transformer oil-based magnetic nanofluid thin layer*", In: J Chem Phys., 2017 Jan 7; 146(1) 014704. doi: 10.1063/1.4973545.